Enabling nanoimprint simulator for quality verification; Process-design co-optimization toward high volume manufacturing

Junichi Seki[1], Yuichiro Oguchi[1], Naoki Kiyohara[1], Koshiro Suzuki[1], Kohei Nagane[1], Shintaro Narioka[2], Takahiro Nakayama[2], Yoshihiro Shiode[2], Sentaro Aihara[2], Toshiya Asano[2]

[1]Canon Inc., 30-2 Shimomaruko 3-chome, Ohta-ku, Tokyo 146-8501, Japan
[2]Canon Inc., 20-2 Kiyohara-Kogyodanchi, Utsunomiya-shi, Tochigi 321-3292, Japan

ABSTRACT

Computational technologies are still in the course of development for nanoimprint lithography (NIL). Only a few simulators are applicable to the nanoimprint process, and these simulators are desired by device manufacturers as part of their daily toolbox. The most challenging issue in NIL process simulation is the scale difference of each component of the system. The template pattern depth and the residual resist film thickness are generally of the order of a few tens of nanometers, while the process needs to work over the entire shot size, which is typically of the order of 10 mm square. This amounts to a scale difference of the order of 10^6. Therefore, in order to calculate the nanoimprint process with conventional fluid structure interaction (FSI) simulators, an enormous number of meshes is required, which results in computation times that are unacceptable. In this paper, we introduce a new process simulator which directly inputs the process parameters, simulates the whole imprinting process, and evaluates the quality of the resulting resist film. To overcome the scale differences, our simulator utilizes analytically integrated expressions which reduce the dimensions of the calculation region. In addition, the simulator can independently consider the positions of the droplets and calculate the droplet coalescence, thereby predicting the distribution of the non-fill areas which originate from the trapped gas between the droplets. The simulator has been applied to the actual NIL system and some examples of its applications are presented here.

Keywords: nanoimprint lithography, NIL, simulation, fluid structure interaction, computation fluid dynamics, CFD, FSI

1. INTRODUCTION

Imprint lithography is an effective and well-known technique for replication of nano-scale structures.[1-3] Nanoimprint lithography (NIL) manufacturing equipment utilizes a patterning technology that involves a field-by-field deposition and an exposure of low viscosity resist droplets dispensed by ink-jetting technology onto the substrate.[3-9] The patterned template is lowered onto the fluid which then quickly flows into the relief patterns in the template by capillary action. Following this filling step, the resist is cured under UV radiation, and then the template is removed, leaving a patterned resist on the substrate. This technology faithfully reproduces patterns with higher resolution and greater uniformity compared to those produced by photolithography equipment. Additionally, as this technology does not require an array of wide-diameter lenses and expensive light sources necessary for advanced photolithography equipment, NIL equipment achieves a simpler, more compact design, allowing multiple units to be clustered together for increasing productivity.

For nanoimprint lithography, computational technologies are still being developed. Only a few simulators are applicable to the nanoimprint process[11-13], and these simulators are desired by device manufacturers as part of their everyday toolbox.[14-16]

Similar to photolithography systems, there are many process parameters to be optimized to achieve greater throughput and better quality of the imprinted patterns. Key physical influencers include the elastic deformation of the template, the rheological behavior and polymerization of the imprint resist under UV exposure, and so on. Therefore, coupling all the influencing physics is mandatory to simulate the imprinting process. For example, the optimization of the dispense pattern of the resist droplets, referred to as the drop-recipe, has a significant effect on the process throughput and the resist uniformity.

Design-Process-Technology Co-optimization for Manufacturability XIV, edited by
Chi-Min Yuan, Proc. of SPIE Vol. 11328, 113280N · © 2020 SPIE
CCC code: 0277-786X/20/$21 · doi: 10.1117/12.2551999

The most challenging issue in NIL process simulation is the scale difference of each component of the system. The template pattern depth and the residual resist film thickness are generally of the order of a few tens of nanometers. Each droplet is spread to a few hundred micrometers in size. The process needs to work over the entire shot size, which is typically of the order of 10 mm square. This creates a scale difference of the order of 10^6. Therefore, in order to calculate the nanoimprint process with conventional fluid structure interaction (FSI) simulators, an enormous number of meshes is required, resulting computation times that are prohibitive.

In this paper, we introduce a new process simulator which directly inputs the process parameters, simulates the whole imprinting process, and evaluates the quality of the resulting resist film. To overcome the scale differences, our simulator utilizes analytically integrated expressions which reduce the dimensions of the calculation region. One of the major features replaces the droplet-template interaction by an analytically solved equation. With this scheme, the process simulator successfully simulates the template movement during the imprinting process. In addition, the simulator can independently consider the positions of the droplets and calculate the droplet coalescence, thereby predicting the distribution of the non-fill areas which originate from the trapped gas between the droplets.

2. NIL PROCESS SIMULATOR

2.1 Overview

The NIL process simulator consists of two complementary simulations: the non-fill defect simulation and the spread simulation as shown in Figure 1. The non-fill defect simulation, which is named as the "global-mode", calculates the resist droplet coalescence and the resulting non-fill areas within the entire shot area. In this simulation, the dynamics of the template is solved simultaneously. Since there is a huge scale difference between the resist droplet and the shot area, the global-mode adopts two different types of meshes for the template and droplets, respectively.

The spread simulation, which is named as the "local-mode", focuses on a fraction of a shot area and calculates the detailed distribution of the film residual layer thickness (RLT). The spread simulation imports and utilizes the template movement profile obtained by the global-mode calculation.

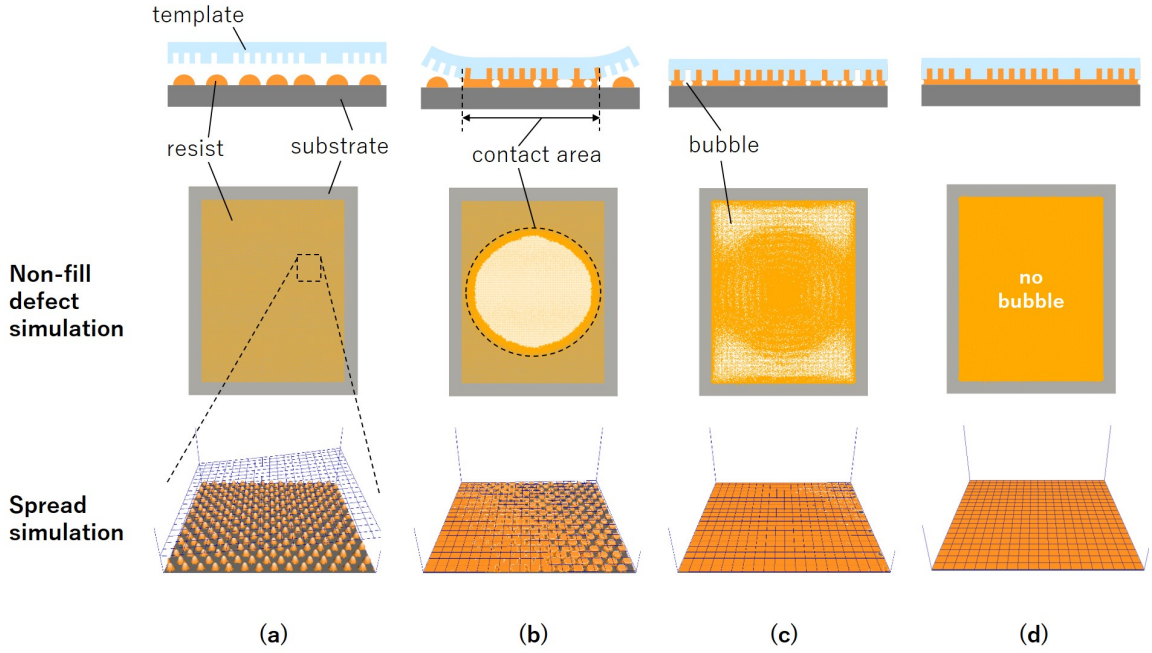

Figure 1. Schematics of the NIL process and the results of the non-fill defect simulation and spread simulation. (a) Resist droplets are dispensed on the substrate. (b) The template contacts the droplets from the center of the shot area and the bubbles (white dots) are temporarily trapped between the droplets. (c) All the droplets coalesce and the bubbles begin to quickly fade away. (d) The bubbles disappear completely about 1.2 seconds after the initial contact.

2.2 Inputs and outputs

The simulator allows the user to directly input many of the parameters specific to the NIL equipment. The schematic of the NIL equipment and the corresponding input parameters are shown in Figure 2. The input parameters include the template patterns, the substrate topography, droplet positions and volumes, which we call "drop-recipe", stamping profile of the imprint head, cavity pressure, etc. The drop-recipe can be generated by our in-house tool, taking into account the template pattern density and the substrate topography. It also requires material properties of the resist, template, substrate, and bubbles.

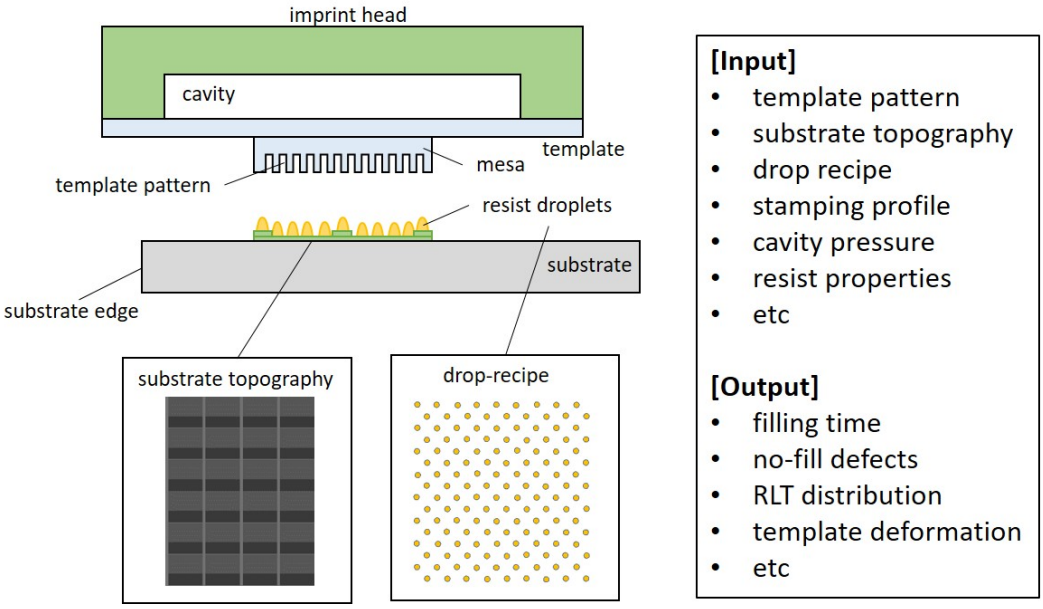

Figure 2. Schematic of NIL equipment and the input parameters for the NIL process simulator.

The global-mode simulation outputs the non-fill defect distribution at each specified time after the imprint starts, the movement and the deformation of the whole template, and the coalescence of the droplets. In the course of the simulation, the gas flow between the droplets, and other physical quantities associated with the imprinting process can be also monitored.

The simulator provides the local-mode simulation to calculate the residual layer thickness (RLT) distribution in more detail. The local-mode requires the result of the global-mode, thus the global-mode must be executed beforehand. This simulation considers local deformations of the template, which would influence RLT distribution. This mode also outputs physical quantities such as resist pressure, resist flux, etc.

2.3 Simulation model

Template dynamics

In order to simulate the NIL process, it is essential to calculate the dynamicsand the deformation of the whole template which is influenced by many physical factors. First, the load is applied to the imprint head to which the template is attached. As the template descends, the template contacts with the resist droplets and receives a counter pressure due to the flow resistance during the droplet spreading. At the same time, the template is also attracted by the surface tension of the resist. While the template approaches, the gas within the gap between the template and the substrate is forced to flow outwards, which yields a counter force. The simulator considers all the physics described above to calculate the template dynamics.

Since the gap between the template and the substrate is extremely small compared with the shot area size, the simulator adopts the lubrication approximation to calculate the fluid (resist and gas) flow within the gap.[13] This enables us to omit meshing along z direction, which reduces the number of meshes significantly. This is one of the major advantages of our simulator against the conventional 3d computational fluid dynamics (CFD) simulators.

Droplet-template interaction

One of the major difficulties of the template dynamics calculation is the evaluation of the droplet counter pressure mentioned above. To calculate such pressure by conventional 3d CFD simulation, one has to resolve each resist droplet by meshes and solve the spreading and coalescence, which requires enormous number of meshes and unacceptable calculation cost. One of the key features of our simulator is to model the droplet-template interaction by analytical expressions. We have analytically integrated fluid flow equation under the appropriate boundary conditions and obtained an expression for each coalescence state. The expressions of the droplet-template interaction are switched according to the state of the droplet coalescence which is calculated in the specific mesh structure (described in the next paragraph). It is no longer required to resolve each droplet, thus one is able to adopt larger meshes where the droplets are represented by number density within each cell. The droplet-template interaction terms are coupled with the template movement and deformation equations.

Droplet coalescences

The simulator can independently take into account the positions of the droplets and calculate the droplet coalescences, thereby predicting the distribution of the non-fill areas which originate from the trapped gas between the droplets. For this purpose, the program utilizes a specific mesh where each node is placed on each droplet. The droplet shape is represented by its rim, therefore there is no mesh within the droplet. The rim shape is updated so as to satisfy the conservation of the resist volume at each time step. The number of meshes is significantly reduced with this scheme, which makes it possible to calculate the droplet coalescence and the bubble trapping within the entire shot area.

In order to predict the non-fill areas at arbitrary time after the imprint starts, it is required to calculate the amount of gas molecules within each bubble, which is proportional to the volume and the gas pressure of the bubble according to the equation of state. The droplets create the gas flow channels towards the outside the shot region, which affects the gas pressure values significantly. Therefore, to obtain the gas pressure distribution between the droplets, it is essential to solve the gas flow simulation over the entire shot area. Furthermore, since the gas pressure and the template dynamics interact with each other, all the above listed factors should be calculated simultaneously, which is also one of the challenging issues in the NIL process simulation.

The above specific mesh is designed to efficiently calculate the bubble volumes and the gas pressure within the bubbles. Conventional simulators require very small meshes to resolve the gas flow channels between the droplets: 5 μm mesh would be required at least. In contrast, our simulator formulates the gas flow equation on this specific mesh structure. The number of the meshes are typically of the order of the number of droplets, which makes it feasible to calculate gas flow over the entire shot region.

2.4 Calculation cost

Our simulator adopts various schemes to reduce the calculation cost as described in 2.3. In this section, we discuss the performance regarding the calculation cost. Table 1 shows the comparison of the calculation time between our simulator and conventional 3d CFD simulators for a typical case of non-fill defect simulation.

Meshing

Conventional 3d CFD simulators require smaller meshes, typically 5 μm as discussed above, to resolve the droplet coalescence and bubble trapping between the droplets. In contrast, our simulator can adopt much larger meshes of typically 500 μm. In addition, adopting the lubrication approximation enables to omit meshes in z direction. Conventional simulators require at least 10 meshes in z direction; otherwise the precision of the flow resistance calculation becomes worse.

Time step and fluid structure interaction algorithm

NIL process involves one of the crucially severe conditions from the point of view of fluid structure interaction (FSI) because tiny change in the z position of the template induces significantly large pressure variation due to the high flow resistance of the narrow gap between the template and the substrate. Conventional CFD simulators typically adopt iterative method with relaxation algorithm to suppress the numerical oscillation during FSI calculation. However, even with this scheme, a very small time step is required for the NIL process simulation. On the other hand, since our simulator adopts the original coupling algorithm for FSI calculation, a much longer time step can be adopted. In addition, our simulator adopts elaborated preconditioned iterative method for solving linear equations[18] which contributes to the further reduction of the calculation time.

Total calculation cost

Our simulator takes 2 to 3 hours for 1 sec calculation with a single thread (without parallel computing). According to the above discussion, the total number of meshes n required for conventional simulators is 10^7 times larger than that of our simulator. If we assume that the calculation time is proportional to $n^{1.3}$, which is typical for conjugate-gradient method for linear equations, the total calculation time is estimated as 2.5×10^5 years. Even if we apply 128 parallel threading, the time only reduces to at least 2200 years which is unacceptable.

Table 1. Comparison of the calculation cost between our simulator and convectional 3d CFD simulators at single core.

	Our simulator	**Conventional 3d CFD**
number of meshes	3432	2.145×10^7
time step	10 us	0.1 us
total calculation time	2 ~ 3 hours	2.5×10^5 years

3. APPLICATION

3.1 Resist spread time versus non-fill defects

In general, shorter spread time is required to realize larger throughput. However, there is a trade-off relation between the spread time and non-fill (bubble) defects. Our simulator can estimate the non-fill defect distribution within the entire shot region at an arbitrary time after the imprint starts. There are various influencing factors for the non-fill defect distribution, such as the drop-recipe, the tool parameters, etc. Applying the simulator enables the user to optimize the above parameters in the early stage of the device development and verify the quality of the resulting resist film, as well as that during the manufacturing process.

In this section, the results of the comparison with the validation measurements are discussed first. Then we demonstrate an example of the drop-recipe optimization for higher throughput and the hot spot detection from the simulation results.

Validation: dependence on the drop-recipe

First we show the results of the basic validation experiments. We compare the simulation results with the measurements for two examples of simple and uniform droplet patterns. For the sake of clarity, we measure the non-fill defects at the early stage of the imprinting process so that there remain many non-fill areas. Figure 3 shows the results of the validation experiments for pattern-A (a) and pattern-B (b), respectively, together with the corresponding simulations. As shown in the figure, our simulator successfully reproduces the measurement tendencies.

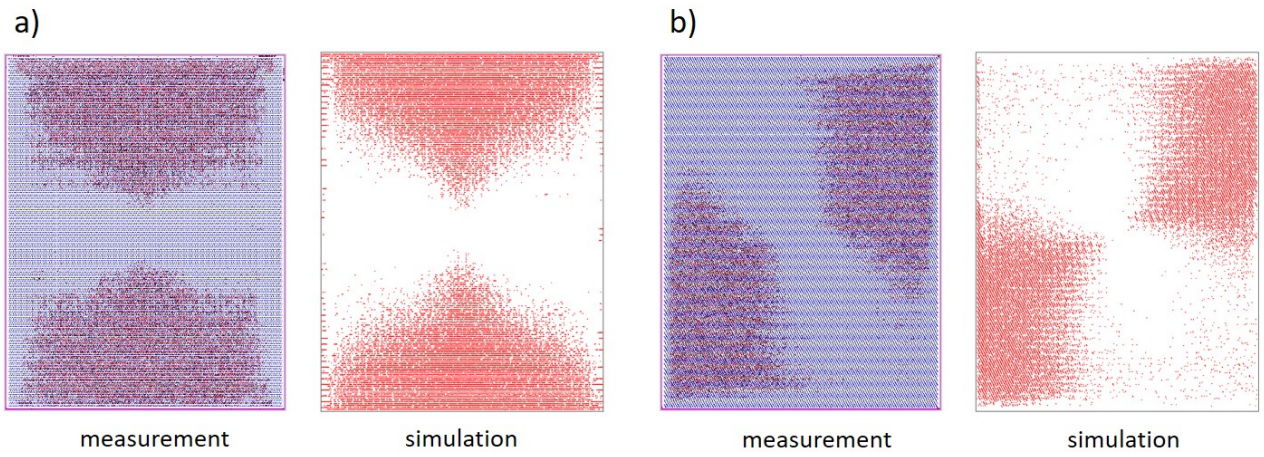

Figure 3. Comparison between the non-fill defect measurements and the corresponding simulation results.

Validation: dependence on the tool parameters

As discussed above, direct input of specific parameters of the NIL equipment is one of the major advantages of our NIL process simulator. We compare the simulations and the measurements for a typical configuration, changing the tool parameter set. Figure 4 shows the results of non-fill defect simulations and the corresponding measurements for (a) the parameter-set A and (b) the parameter-set B, where the results are compared at short spread time for the sake of clarity. The simulator is now able to successfully estimate the imprint result without any trial manufacturing.

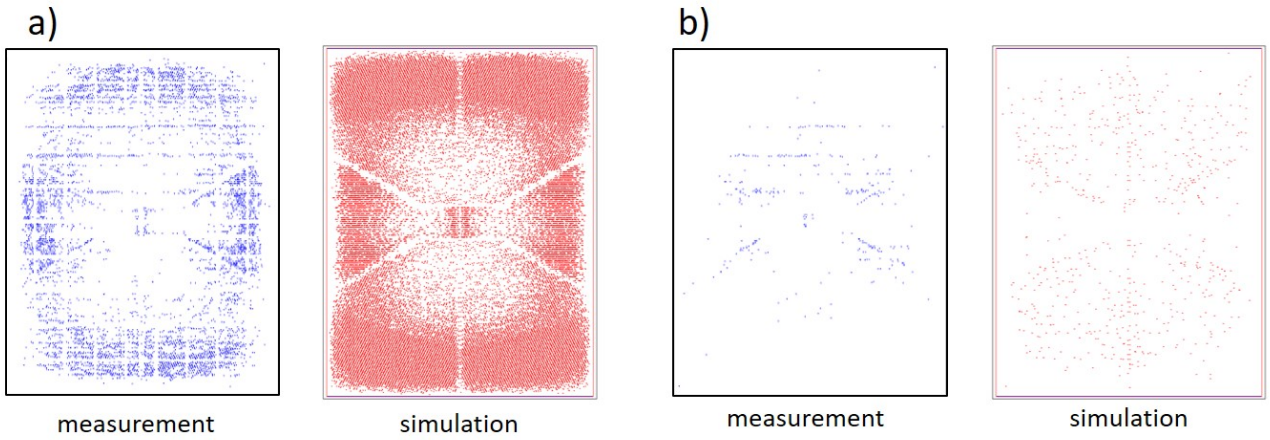

Figure 4. Comparison between the simulations and the measurements for (a) parameter-set A and (b) parameter-set B.

Optimization of drop-recipe for higher throughput

As discussed above, the gas pressure between the template and the substrate is one of the key influencing factors for the spread time. The configuration of the gas flow channel strongly depends on how the droplets are coalesced with each other. Therefore, controlling the direction of the droplet coalescence enables us to realize suppressed gas pressure and, in turn higher throughput.

We have optimized the drop-recipe and evaluated the impact of this scheme by our simulator. Figure 5 shows the calculation results of the non-fill defect simulation for (a) the original uniform drop-recipe and (b) the optimized drop-recipe, where red dots represent the non-fill defects. One can see that the non-fill defects disappear significantly faster in the optimized-recipe. Our simulator is already in use to optimize droplet patterns without any trial manufacturing.

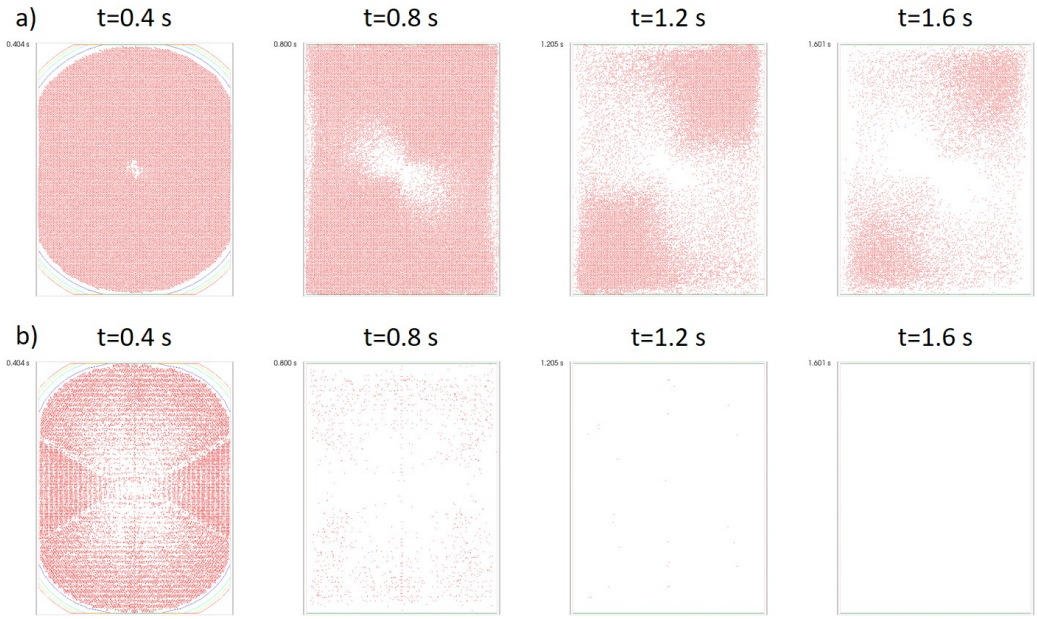

Figure 5. Comparison of the non-fill defects for (a) the uniform-recipe and (b) the optimized-recipe at t = 0.4, 0.8, 1.2, 1.6 sec. The red dots represent the non-fill defects.

Hot spot detection

The global-mode of the NIL process simulator provides us with the droplet coalescence behavior of the entire shot region, where the droplet pattern, the substrate topography, and the template pattern density are taken into account. From the simulation results, the user can identify hot spots where non-fill defects are likely to appear.

Here we demonstrate an example of hot spot detection using our simulator. Figure 6 shows two snapshots of the non-fill defect simulation, where the contact area of the template and the resist appears from the left side and proceeds to the right side. As the template approaches the substrate, the droplets located on the convex line coalesces earlier and seals the gas flow channels outwards of the shot region. Then a substantial amount of gas is trapped within a large area which stretch adjacent to the convex line, which is enclosed by a red solid line in Figure 6. Therefore many non-fill defects are expected to appear in this area, which is thus considered to be a hot spot.

Various means are available to avoid this hot spot. Here we show two examples. The first is to flatten the substrate topography by optimizing preprocesses, which is expected to be effective since the difference in the depth of the topography is the root cause of the above hot spot. The second is to add droplets around the hot spot. Additional droplets would reduce the droplet pitch and coalescence is expected to proceed faster, which would avoid the gas channel sealing by the droplets on the convex line.

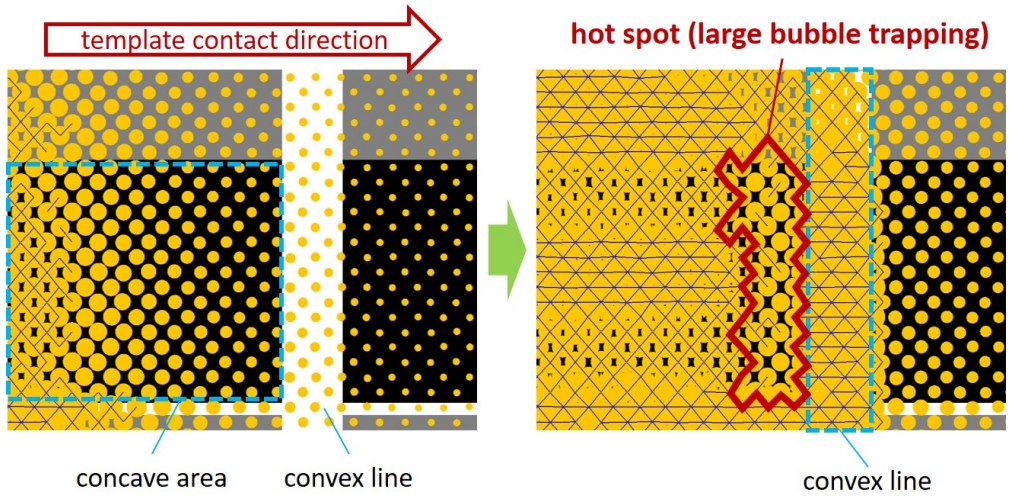

Figure 6. Example of hot spot detection by the global-mode simulation where orange filled circles represent the droplets, the grey-scale background represents the substrate topography, solid black lines represent the linkage between the droplets which coalesce with each other.

3.2 Residual layer thickness (RLT) distribution

The local residual layer thickness (RLT) and the film surface height is affected by the drop-recipe, the template pattern, and the substrate topography. Our simulator is able to calculate local RLT distribution, taking into account the factors listed above. The resist film flatness is one of the key influencing factors regarding the overlay accuracy, thus optimization is required.

There would be two major means to acquire sufficient RLT control. One is to reduce the substrate topography by optimizing the pre-processes. The other is to optimize the drop-recipe. We apply our simulator to demonstrate the impact of these measures, and we show some examples below.

Calculation condition

A dummy substrate topography and template patterns are prepared which are illustrated in Figure 7. The maximum depth of the substrate topography is 30 nm. The vertical convex line is 500 μm wide and the horizontal one is 100 μm wide. The pattern density is 0% on the convex areas, while it is 25% and 10% in the areas enclosed by dotted lines and dashed lines, respectively. The above substrate and the template structure is repeated over the shot region 26mm×33mm. First we simulate the entire template dynamics (global-mode) and then perform the detailed spread simulation (local-mode) for the 4mm×4mm area depicted by a thick solid line in Figure 7 (b).

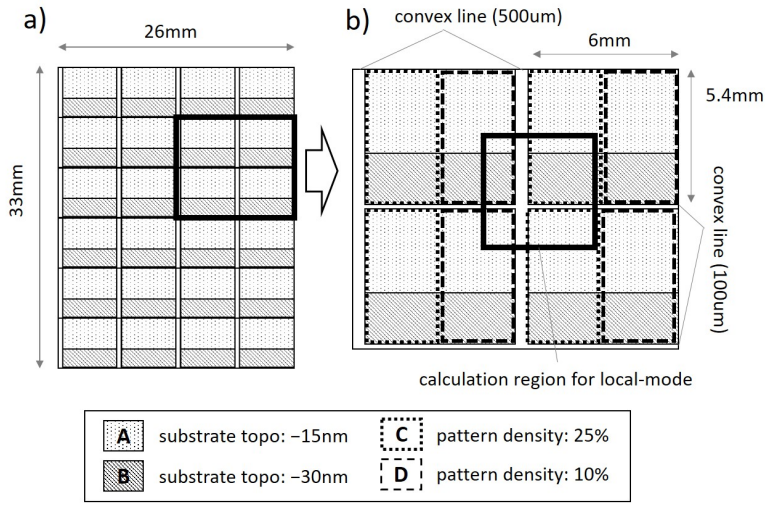

Figure 7. Schematic of the calculation condition: substrate topography and template pattern densities.

Results and discussions

Figure 8 (a) shows the result of the local-mode simulation for the uniform drop-recipe. The resist film surface is depicted as 3d deformed surface colored by its z coordinate. The maximum gap between the top and the bottom is about 40 nm, where the resist film surface swells around the vertical convex line which is 500 μm wide. The difference of the film surface height observed on both sides between the vertical line can be attributed to the template pattern density: 10% for the left-side and 25% for the right-side.

If we manage to reduce the substrate topography from 30 nm to 10 nm, we can expect that the flatness of the film would be improved. Figure 8 (b) shows the corresponding simulation result where maximum depth is reduced to about 20 nm. It surely improves the film surface flatness, although there still remains the large gap of 20 nm, which corresponds to the flatness σ of 6.5 nm. This indicates that the substrate topography reduction is not sufficient to compensate the pattern density difference.

Then the drop-recipe is optimized considering both the substrate topography and the template pattern density. The corresponding result of the local-mode simulation is shown in Figure 8 (c). We can see that satisfactory flatness is realized and the flatness σ is now reduced to 1.1 nm. The above results are summarized in the chart in Figure 8 (d).

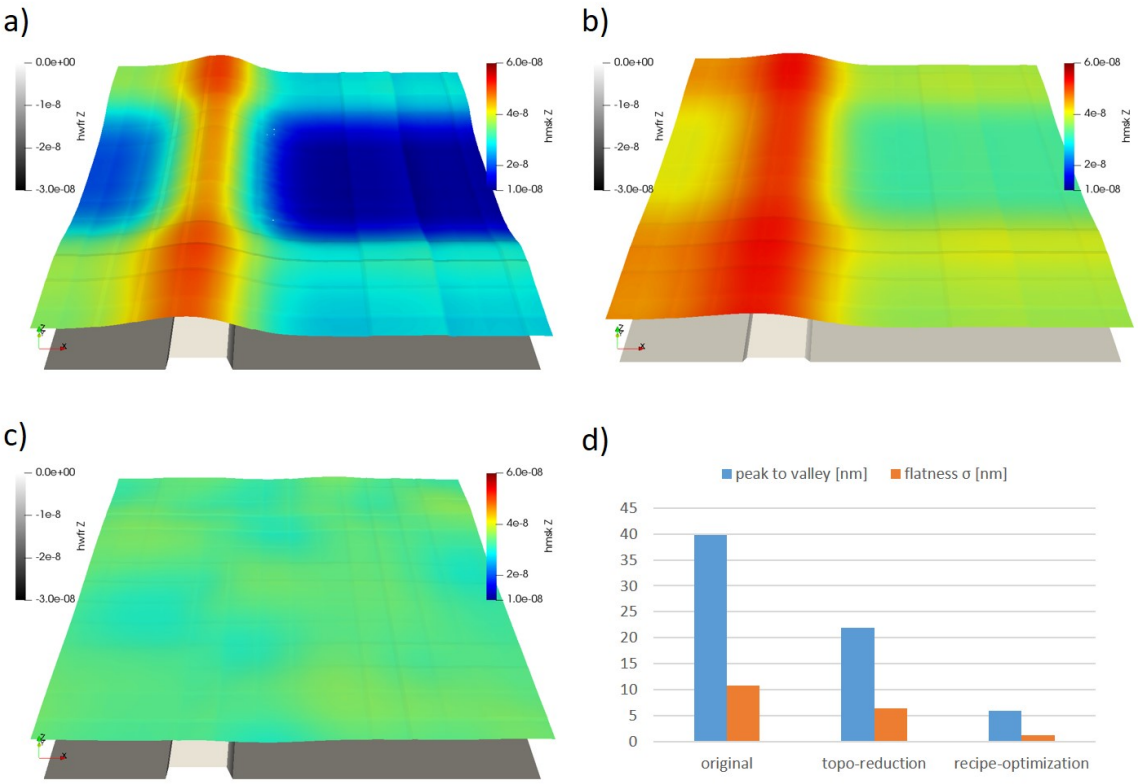

Figure 8 Spread simulation results of (a) the original configuration, (b) the reduced substrate topography and (c) the optimized drop-recipe. The peak to valley values of the film surface and the flatness σ are shown in (d).

3.3 Distortion

Importance of RLT control on OL accuracy

Overlay (OL) accuracy is one of the most important factors in manufacturing. To obtain better OL accuracy, various means are applied such as HODC[19]. It is reported that RLT uniformity is also an important factor for higher overlay accuracy, since the region of thin resist film thickness yields high shear stress during the alignment process and would induce large distortion[17].

Drop pattern compensation[20] is one of the promising measures to obtain better flatness of the resist film surface and increased overlay accuracy. The idea of the method is to modify the droplet pattern so as to compensate the local mismatch between the resist volume and the gap space between the template and the substrate. If overlay distortion distribution is measured once, then an ideal RLT distribution is evaluated so that the induced surface deformations compensates the measured distortions. Then additional droplets required for the above obtained RLT distribution is calculated. For the updated drop-recipe, OL accuracy measurement is repeated again and improved distortion map is updated. This process is iterated until the OL accuracy meets the criteria.

To improve the above modification process of the drop-recipe, the user desires to know the resulting resist film surface deformations due to the droplet pattern modification. The NIL process simulator is already capable of simulating the resulting film surface topography as discussed below.

Calculation condition

First, droplets are uniformly located with a number density which corresponds to 30 nm film thickness. Then additional droplets with the same number density are placed within a region of 1 mm square and 2 mm square, respectively. Therefore 60 nm film thickness is expected to be obtained within the square regions.

Results and discussions

Figure 9 shows the results of the local-mode simulation where the color contour represents the film height. The black circles represent the initial droplet positions. The additional droplets are located on the area surrounded by thick dashed lines. The solid blue lines in the bottom figures represent the cross section of the resist film. The orange dashed lines represent the naive expectations of the film thickness distribution according to the droplet configuration. We can see that the distribution of the resist film thickness has a slope with a finite width (about 0.5 mm). For (a) the case of smaller area of additional droplets, there is no plateau within the added area. For (b) the case of larger additional droplet area, a plateau region is observed around the center.

The above deviations from the naive expectations and the actual resist film thickness would influence the DPC process significantly. If we could know the distribution of the actual film thickness beforehand by this simulation, it is possible to optimize the additional droplet patterns to compensate the observed distortions.

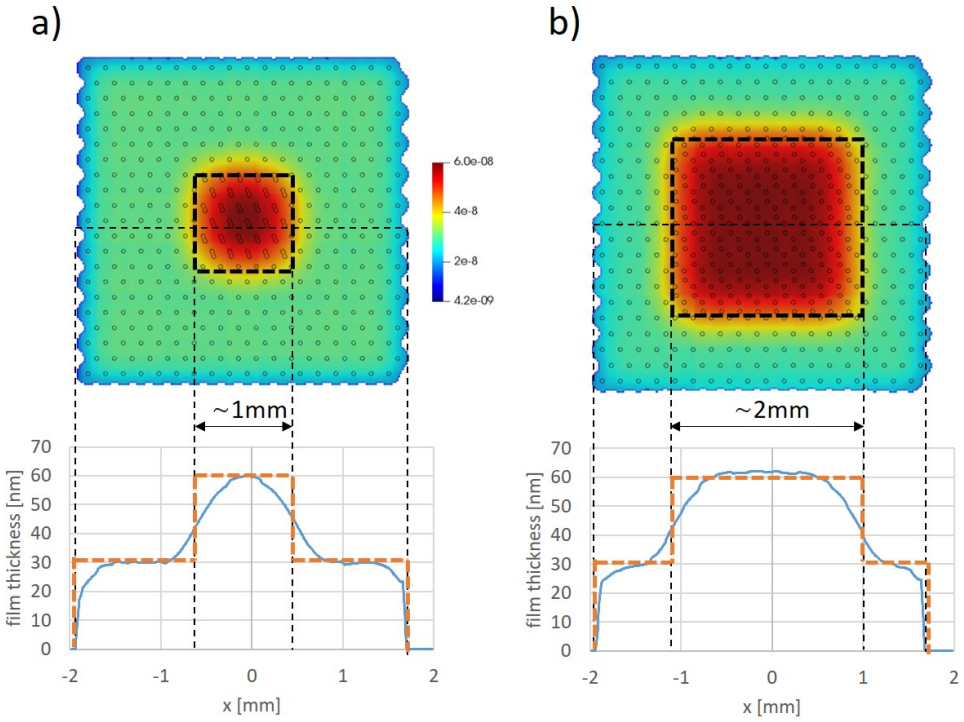

Figure 9. RLT distribution obtained by local-mode simulation.

4. CONCLUSION

In this paper, we describe the details and demonstrate the advantages of the simulation model. Our simulator adopts various schemes to reduce calculation cost and succeeds to simulate the NIL imprinting process of the entire shot region which cannot be achieved by conventional 3d CFD simulators. The simulator has already been applied to process-design optimization and we show some application examples.

REFERENCES

[1] S. Y. Chou, P. R. Kraus, P. J. Renstrom, “Nanoimprint Lithography”, J. Vac. Sci. Technol. B 1996, 14(6), 4129 - 4133.

[2] S.Fujimori, Jpn. J. Appl. Phys. 48(6), 06FH01 (2009).
[3] T. K. Widden, D. K. Ferry, M. N. Kozicki, E. Kim, A. Kumar, J. Wilbur, G. M. Whitesides, Nanotechnology, 1996, 7, 447 - 451.
[4] M. Colburn, S. Johnson, M. Stewart, S. Damle, T. Bailey, B. Choi, M. Wedlake, T. Michaelson, S. V. Sreenivasan, J. Ekerdt, and C. G. Willson, Proc. SPIE, Emerging Lithographic Technologies III, 379 (1999).
[5] M. Colburn, T. Bailey, B. J. Choi, J. G. Ekerdt, S. V. Sreenivasan, Solid State Technology, 67, June 2001.
[6] T. C. Bailey, D. J. Resnick, D. Mancini, K. J. Nordquist, W. J. Dauksher, E. Ainley, A. Talin, K. Gehoski, J. H. Baker, B. J. Choi, S. Johnson, M. Colburn, S. V. Sreenivasan, J. G. Ekerdt, and C. G. Willson, Microelectronic Engineering 61-62 (2002) 461-467.
[7] S.V. Sreenivasan, P. Schumaker, B. Mokaberi-Nezhad, J. Choi, J. Perez, V. Truskett, F. Xu, X, Lu, presented at the SPIE Advanced Lithography Symposium, Conference 7271, 2009.
[8] K. Selenidis, J. Maltabes, I. McMackin, J. Perez, W. Martin, D. J. Resnick, S.V. Sreenivasan, Proc. SPIE Vol. 6730, 67300F-1, 2007.
[9] I. McMackin, J. Choi, P. Schumaker, V. Nguyen, F. Xu, E. Thompson, D. Babbs, S. V. Sreenivasan, M. Watts, and N. Schumaker, Proc. SPIE 5374, 222 (2004).
[10] K. S. Selinidis, C. B. Brooks, G. F. Doyle, L. Brown, C. Jones, J. Imhof, D. L. LaBrake, D. J. Resnick, S. V. Sreenivasan, Proc. SPIE 7970 (2011) 797009.
[11] H. Taylor, Y. C. Lam, D. Boning, J. Micromech. Microeng. 19 (2009).
[12] H. Taylor, D. Boning, Proc. SPIE 7641 (2010) 76410U.
[13] H. K. Taylor, Proc. SPIE 9777 (2016) 97770E.
[14] S. Kobayashi, M. Komori, R. Inanami, K. Yamashita, A. Mimotogi, J. Y, Im, M. Hatano, T, Kono, S. Maeda, Proc. SPIE 9777 (2016) 977708.
[15] S. Kobayashi, R. Inanami, H. Tsuda, K. Washida, M. Komori, K. Yamashita, J. Y. Im, T. Kono, S. Maeda, Proc. SPIE 10144 (2017) 101440X.
[16] S. Kobayashi, K. Yamashita, H. Tsuda, K. Washida, M. Komori, J. Y. Im, T. Kono, T. Nakasugi, Proc. SPIE 10584 (2018) 105840R.
[17] K. Fukuhara, M. Suzuki, M. Mitsuyasu, T. Kono, T. Nakasugi, Y. Lim, W. Jung, Proc. SPIE 10144 (2017) 1014409
[18] Y. Miki and T. Washizawa, SIAM J. Sci. Comput., 35(2), A1212–A1232
[19] Y. Takabayashi, T. Iwanaga, M. Hiura, H. Morohoshi, T. Hayashi, and T. Komaki, Proc. SPIE 10958 (2019) 109580B
[20] A.Cherala et al, Proc. SPIE 10958 (2019) 109580C